RNA-specific Adenosine Deaminase ADAR1 Suppresses Measles Virus-induced Apoptosis and Activation of Protein Kinase PKR*

Ann M. Toth[‡], **Zhiqun Li**[§], **Roberto Cattaneo**[¶], and **Charles E. Samuel**[‡§1]

From the ‡Department of Molecular, Cellular, and Developmental Biology and the §Biomolecular Science and Engineering Program, University of California, Santa Barbara, California 93106 and the ¶Department of Molecular Medicine and Virology, Mayo Clinic College of Medicine, Rochester, Minnesota 55905

ADAR1 (adenosine deaminase acting on RNA) catalyzes the conversion of adenosine to inosine, a process known as A-to-I editing. Extensive A-to-I editing has been described in viral RNAs isolated from the brains of patients persistently infected with measles virus, although the precise role of ADAR during measles virus infection remains unknown. We generated human HeLa cells stably deficient in ADAR1 ("ADAR1[kd] cells") through short hairpin RNA-mediated knockdown, and using these cells, we tested the effect of ADAR1 deficiency on measles virus (MVvac strain) growth and virus-induced cell death. We found that the growth of mutant viruses lacking expression of the viral accessory proteins V and C (V[ko] and C[ko], respectively) was decreased in ADAR1-deficient cells compared with ADAR1-sufficient cells. In addition, apoptosis was enhanced in ADAR1-deficient cells following infection with wild type and V[ko] virus but not following infection with C[ko] virus or treatment with tumor necrosis factor-α or staurosporine. Furthermore, in C[ko]-infected ADAR1-sufficient cells when ADAR1 did not protect against apoptosis, caspase cleavage of the ADAR1 p150 protein was detected. Finally, enhanced apoptosis in ADAR1[kd] cells following infection with wild type and V[ko] virus correlated with enhanced activation of PKR kinase and interferon regulatory factor IRF-3. Taken together, these results demonstrate that ADAR1 is a proviral, antiapoptotic host factor in the context of measles virus infection and suggest that the antiapoptotic activity of ADAR1 is achieved through suppression of activation of proapoptotic and double-stranded RNA-dependent activities, as exemplified by PKR and IRF-3.

ADAR1 (adenosine deaminase acting on RNA) is an RNA-specific C-6 adenosine deaminase that catalyzes the conversion of adenosine (A) to inosine (I) on RNAs with double-stranded character (1, 2). Such "A-to-I editing" by ADAR1 is of broad biologic importance, because I is recognized as G instead of A by ribosomes and polymerases (2, 3). For example, ADAR1 plays an important role in the nervous system, where site-specific editing of glutamate receptor and serotonin-2C receptor pre-mRNAs changes their coding capacity, thereby leading to neurotransmitter receptor protein products with altered physiological properties (4–6). In addition, ADAR1 is involved in the RNA interference pathway and is known to alter both the targeting and the processing of microRNAs (7, 8). Furthermore, RNA editing patterns characteristic of ADAR enzymes have been detected in several viral RNAs, including those of measles virus (9, 10), influenza virus (11), lymphocytic choriomeningitis virus (12), polyomavirus (13), hepatitis delta virus (14), and hepatitis C virus (15).

ADAR1 is encoded by a single-copy gene that maps to human chromosome 1q21 (16, 17). The domain structure of the ADAR1 protein product includes the C-terminal deaminase catalytic domain, three centrally located dsRNA[2] binding domains, and one or two N-terminal Z-DNA binding domains (18–20). Two size forms of the ADAR1 protein are known (18, 21, 22). One, p110, is constitutively expressed and found predominantly in the nucleus of cells; the other, p150, is interferon (IFN)-inducible and is found in both the nucleus and the cytoplasm. Compared with p110, the p150 form of human ADAR1 possesses an additional 295 N-terminal amino acids. The function of the N-terminal extension of p150 is not entirely understood, but the region contains a nuclear export signal (23) and an additional Z-DNA binding domain (19). Because of its regulation by IFN and cytoplasmic localization, the p150 version of ADAR1 is thought to be the form responsible for the A-to-I editing of viral RNAs produced by viruses that replicate in the cytoplasm of infected cells (2, 3).

Measles virus (MV), a member of the *Morbillivirus* genus of the family *Paramyxoviridae*, is a negative-stranded RNA virus whose replication cycle takes place entirely in the host cell cytoplasm (24). MV causes an acute respiratory illness in humans, and despite effective vaccination, MV continues to be a pathogen of major global importance (24). In rare cases, the acute infection can lead to a persistent central nervous system infection, resulting in a chronic and fatal disease known as subacute

[2] The abbreviations used are: dsRNA, double-stranded RNA; ADAR1[kd], ADAR1 knockdown cells; C[ko], C knockout measles virus; CON[kd], control knockdown cells; eIF-2α, eukaryotic translation initiation factor-2α; IFN, interferon; MTS, 3-(4,5-dimethylthiazol-2-yl)-5-(3-carboxymethonyphenol)-2-(4-sulfophenyl)-2H-tetrazolium; MV, measles virus; PARP, poly(ADP-ribose) polymerase; PKR[kd], PKR knockdown cells; shRNA, short hairpin RNA; SSPE, subacute sclerosing panencephalitis; TCID$_{50}$, 50% tissue culture infectious dose; TNF-α, tumor necrosis factor-α; V[ko], V knockout measles virus; WT, wild type; GFP, green fluorescent protein; z, benzyloxycarbonyl; fmk, fluoromethylketone.

sclerosing panencephalitis (SSPE) (25). Analysis of viral RNA from SSPE autopsies reveals extensive A-to-I hypermutation in the matrix gene and several other virus genes (10, 26, 27), implicating a role for ADAR during MV infection. However, the effects of ADAR enzymes on the infectious cycle of MV remain largely unknown.

To investigate the role of ADAR1 during MV infection, we used an shRNA-mediated knockdown strategy to create a human HeLa cell line stably deficient in ADAR1 expression. This cell line, called ADAR1^{kd}, was then used to study the effects of ADAR1 on virus growth and cell killing induced by MVvac, a recombinant MV based on the Moraten vaccine strain. The results obtained with the parental MVvac were compared with those of derived isogenic mutant viruses lacking expression of either the V or C accessory protein. Because ADAR1 is an interferon-inducible enzyme and because biased hypermutation such as that observed in SSPE appears to be detrimental to MV, we predicted that MVvac, or at least the V or C mutants of this virus, would grow to higher titers in the ADAR1^{kd} cells compared with parental controls. However, we found the opposite, that ADAR1 acts as a proviral host factor in the context of MV infection and functions to enhance virus growth and suppress virus-induced cell death. Moreover, the mechanism of ADAR1 enhancement of virus growth and suppression of virus-induced cell death is consistent with impairment of dsRNA-mediated innate antiviral responses, exemplified by those of PKR (protein kinase regulated by RNA) and IRF-3 (interferon regulatory transcription factor-3).

EXPERIMENTAL PROCEDURES

Cells and Viruses—Parental HeLa and Vero cells were maintained in Dulbecco's modified Eagle's medium supplemented with 5% (v/v) fetal bovine serum (HyClone), 100 μg/ml penicillin, and 100 units/ml streptomycin (Invitrogen), as described previously (28). HeLa cells with the stable knockdown of PKR (PKR^{kd}) (29, 30) or ADAR1 (ADAR1^{kd}; see below) by RNA interference were maintained in the above-named medium containing 1 μg/ml puromycin (Sigma). Treatment with TNF-α (Sigma) was carried out at the indicated concentrations and times together with 1 μg/ml cyclohexamide. Treatment with staurosporine (Chemicon) was carried out with the indicated concentrations and times. Treatment with the pancaspase inhibitor benzyloxycarbonyl-Val-Ala-Asp-fluoromethylketone (z-VAD-fmk; EMD/Calbiochem) was with a concentration of 100 μM beginning after the virus inoculum was removed.

The recombinant parental MVvac GFP(H) virus, herein designated as wild type (WT), as well as V-deficient (V^{ko}) and C-deficient (C^{ko}) versions of this virus were constructed based on the Moraten vaccine strain, as described previously (28, 31).

Construction of shRNA Expression Vector Plasmid—The pSUPER.retro.puro vector with H1 promoter (Oligo Engine) was used for construction of short hairpin expression constructs to silence human ADAR1. The successful 21-nucleotide human ADAR1 targeting sequence (5'-GTTGACTAA-GTCACATGTAAA-3') present in the 3'-untranslated region of human ADAR1 (18) was identified using Promega online software. The sense strand oligonucleotide (5'-GAT-

CCCC<u>GTTGACTAAGTCACATGTAAA</u>TTCAAGAGA<u>TT-TACATGTGACTTAGTCAAC</u>TTTTTA-3') and antisense-strand oligonucleotide (5'-AGCTTAAAAA<u>GTTGACTAAG-TCACATGTAAA</u>TCTCTTGAA<u>TTTACATGTGACTTAG-TCAAC</u>GGG-3') shown with the targeting sequence underlined were annealed, and the resulting duplex was inserted into the pSUPER.retro.puro vector using the HindIII and BglII restriction sites. Recombinant plasmid constructs were verified by DNA sequence analysis.

Cell Transfection—HeLa cells were transfected at 80–90% confluence using Lipofectamine 2000 (Invitrogen) according to the manufacturer's recommendations. Briefly, Lipofectamine 2000 and plasmid DNA were diluted and mixed in Opti-MEM (Invitrogen), the DNA-Lipofectamine 2000 complexes were applied to the cultures, and incubation continued for 4 h at 37 °C, after which the transfection medium was replaced with fresh maintenance medium containing 5% (v/v) fetal bovine serum. To select for stable transfectants, cells were trypsinized 24 h after transfection with the shRNA pSUPER.retro.puro construct, seeded at various dilutions, and then carried in the presence of 1 μg/ml puromycin. Puromycin-resistant clones were isolated and screened by Western immunoblot analysis for ADAR1 protein knockdown. HeLa cells transfected with the pSUPER.retro.puro vector with H1 promoter without shRNA-encoded insertion were selected and maintained in the puromycin-containing medium. These cells, called CON^{kd} (formerly called PKR^{kd-con} (28)), were used as an additional PKR- and ADAR1-positive control.

Virus Infections and Growth Assays—ADAR1^{kd}, CON^{kd}, and/or ADAR1$^+$ cells were infected at a multiplicity of infection of 5 TCID$_{50}$/cell for the indicated amounts of time, as indicated throughout. Virus yields were determined by 50% TCID$_{50}$ titration on Vero cells according to the Spearman-Karber method (28, 32).

Western Immunoblot Analysis—Whole cell extracts were prepared at the indicated times postinfection, and protein concentrations were determined as described previously (28). Proteins were fractionated by SDS-PAGE and transferred to nitrocellulose, and the membranes were blocked in 5% milk in phosphate-buffered saline. Rabbit polyclonal antibodies against measles virus proteins were described previously (28). Rabbit polyclonal antibody against ADAR1 (K88#2) was described previously (18). Rabbit polyclonal antibodies from the indicated sources were used to detect GFP (Santa Cruz Biotechnology), human PKR (Santa Cruz Biotechnology), IRF-3 (Santa Cruz Biotechnology), phospho-Thr^{446}-PKR (Santa Cruz Biotechnology and Epitomics), and phospho-Ser^{51}-eIF-2α (Cell Signaling). Mouse monoclonal antibodies were used to detect β-actin (Sigma) and human poly(ADP-ribose) polymerase (PARP) (BD Biosciences).

Cell Viability Assays—The MTS colorimetric assay (Promega) was performed according to the manufacturer's instructions. This assay is based on the conversion of the MTS tetrazolium salt into soluble formazan by endogenous dehydrogenase enzymes found in metabolically active cells. Cells were plated at 2.5×10^4 cells/well in 96-well plates. The following day, cells were infected with WT, V^{ko}, or C^{ko} virus or treated with TNF-α/cyclohexamide or staurosporine as indi-

cated. Following infection or treatment, 20 μl of MTS was added, followed by a 1-h incubation at 37 °C, after which the absorbance was measured at 490 nm on a Victor³V plate reader (PerkinElmer Life Sciences).

RESULTS

ADAR1 Enhances the Growth of Measles Virus—To test the effect of ADAR1 on MV infection, we utilized a HeLa clonal line in which ADAR1 expression is stably knocked down by RNA interference. These ADAR1^kd cells have less than 15% of the p110 form and less than 10% of the p150 form of ADAR1 found in either parental HeLa cells (ADAR1^+) or drug-treated control cells (CON^kd) (data not shown) (see Figs. 2C and 3B). We used the recombinant MVvac strain and isogenic V^ko and C^ko mutants of this virus. All of these viruses encode a GFP gene downstream of the hemagglutinin gene, and since MVvac is a vaccine lineage strain, these viruses can enter through CD46 (cluster of differentiation 46) (33), a receptor expressed on ADAR1-deficient and -sufficient HeLa cell lines.

We examined the growth of MVvac WT and mutant recombinant MV in ADAR1-deficient (ADAR1^kd) and ADAR1-sufficient (ADAR1^+ and CON^kd) human cell lines, both qualitatively (Fig. 1A) and quantitatively (Fig. 1B). As previously observed for PKR-sufficient cells (28), the GFP reporter signal viewed by fluorescence microscopy was high for WT and V^ko but low for C^ko in parental HeLa (ADAR1^+) and drug control (CON^kd) cells (Fig. 1A). However, in ADAR1^kd cells, the GFP signal for all three viruses was very low (Fig. 1A), suggesting that these viruses grew poorly in the absence of ADAR1. To quantify the growth of virus, infectious virus yields were determined on Vero cells. When grown in ADAR1^+ parental HeLa cells and CON^kd drug control cells (28), the yield of the C^ko virus was about 30-fold lower than the WT virus, whereas the yield of V^ko was similar to the WT virus (Fig. 1B), consistent with earlier findings (28). The yields of the V^ko and C^ko viruses, however, were significantly reduced in ADAR1^kd cells compared with ADAR1-sufficient cells, about 8- and 12-fold, respectively (Fig. 1B). These results suggest that ADAR1 enhances the growth of measles virus.

ADAR1 Suppresses WT and V^ko Virus-induced Apoptosis— While determining MV growth in ADAR1-sufficient and ADAR1-deficient cells, we observed greater cytopathic effect after infection of ADAR1^kd compared with ADAR1^+ or CON^kd cells with WT and especially V^ko virus, as illustrated by the phase-contrast images shown in Fig. 2A.

To quantify the effect, the colorimetric MTS assay was employed. The MTS assay revealed that the number of viable ADAR1^kd cells was indeed decreased compared with the numbers of viable ADAR1^+ or CON^kd cells following infection with WT and V^ko virus (Fig. 2B). Although the C^ko virus was far more cytopathic than either WT or V^ko (Fig. 2, A and B), which is consistent with our prior observations in ADAR1-sufficient cells (28), the cell killing capacity of C^ko, however, was not further enhanced in ADAR1^kd cells (Fig. 2B). We showed previously that the MV-induced cytopathic effect observed by microscopy correlated well with cleavage of the caspase substrate PARP and was therefore probably apoptotic (28). We thus performed western immunoblot analysis with an anti-
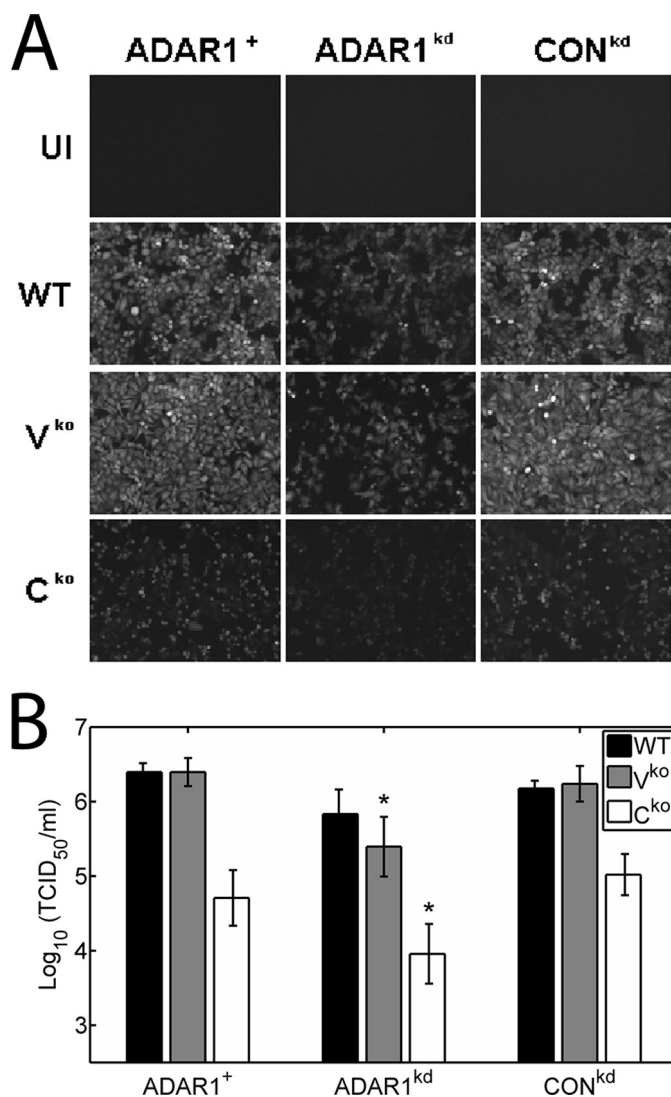

FIGURE 1. **Growth of wild type and V- and C-mutant measles virus in ADAR1-deficient and ADAR1-sufficient cells.** ADAR1^+, ADAR1^kd, and CON^kd HeLa cells were infected with WT, V^ko, or C^ko recombinant virus at a multiplicity of infection of 5 TCID$_{50}$/cell for 36 h. *A*, fluorescence images showing GFP signal in cells taken immediately before harvest. *UI*, uninfected cells. *B*, virus yields from ADAR1-sufficient (parental ADAR1^+ and CON^kd) and stably ADAR1-deficient (ADAR1^kd) cells were determined by 50% TCID$_{50}$ titration on Vero cells. The results shown are the means with S.D. ($n = 4$). *, $p < 0.05$ by Student's *t* test for comparison of V^ko and C^ko virus yields in ADAR1^kd cells *versus* ADAR1-sufficient controls.

PARP antibody to further assess the cell killing in ADAR1^kd *versus* ADAR1-sufficient controls. As reported previously for parental HeLa cells and drug control cells (28), the PARP cleavage was most pronounced following infection with the C^ko virus and least with the WT virus (Fig. 2C). In the ADAR1^kd cells compared with the ADAR1-sufficient cells, the PARP cleavage following infection with WT and especially V^ko virus was greatly enhanced. However, apoptosis following infection with C^ko virus was not enhanced by the ADAR1 deficiency.

ADAR1 Does Not Protect against TNF-α- or Staurosporine-induced Apoptosis—Double-stranded RNA is potentially the trigger for apoptosis in MV-infected cells, since MV-induced apoptosis is mediated at least in part by PKR (28), a protein kinase that is activated upon binding structured RNA or
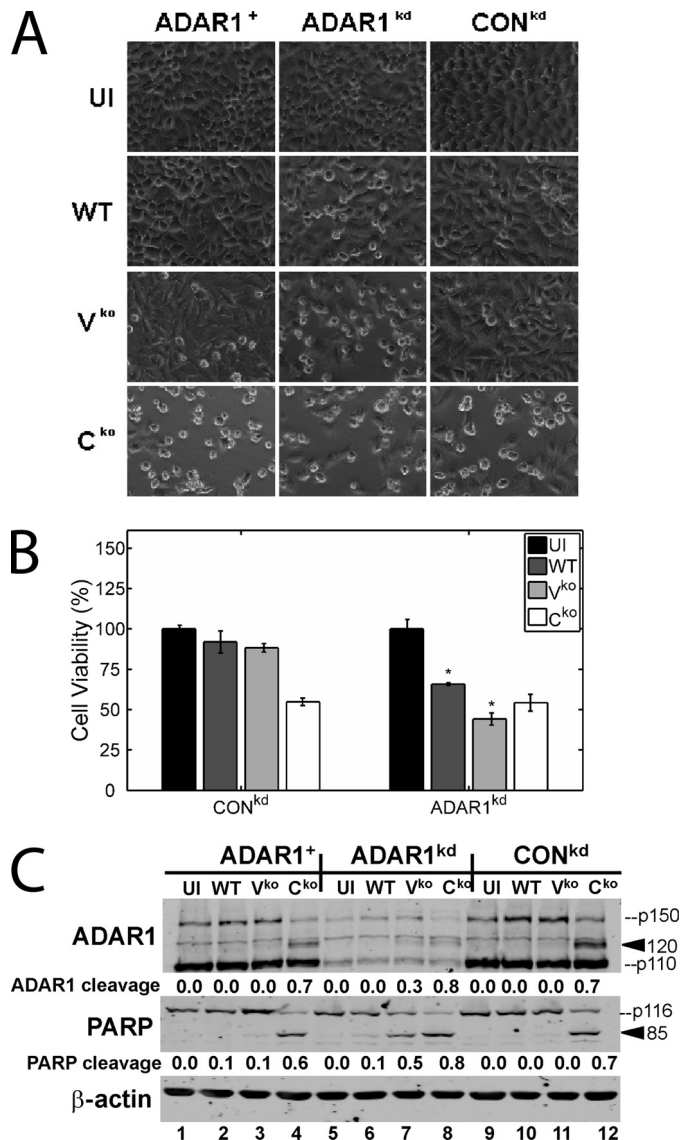
FIGURE 2. **Measles virus-induced apoptosis is enhanced in ADAR1-deficient cells and ADAR1 is cleaved by caspases during MV infection.** ADAR1^{+}, ADAR1[kd], and CON[kd] HeLa cells were left uninfected (*UI*) or infected with WT, V[ko], or C[ko] recombinant virus for 36 h. *A*, phase-contrast images taken immediately before harvest. *B*, results of the colorimetric MTS assay to measure cell viability 36 h postinfection, displayed as percentages of the number of viable uninfected cells with S.D. (*n* = 4). *, $p < 0.005$ by Student's *t* test for comparison of the C[ko] virus yields in ADAR1[kd] cells and those in ADAR1^{+} or CON[kd] cells. *C*, Western immunoblot analyses performed on whole cell extracts using antibodies against ADAR1, PARP, and β-actin. The quantity of PARP cleavage based on the immunoblots, expressed as a ratio of the 85-kDa cleavage product to total PARP (85/(85 + p116)), is shown *below* each *lane*. Likewise, the quantity of ADAR1 cleavage based on the immunoblots, expressed as a ratio of the 120-kDa cleavage product to total ADAR1 (120/(120 + p150)), is shown *below* each *lane*. The *arrowheads* mark the positions of the PARP 85 and ADAR1 120 cleavage products.

dsRNA. Because ADAR1 suppresses MV-induced apoptosis (Fig. 2) and because ADAR1 binds dsRNA (18) and was discovered based on its dsRNA-unwinding activity (34, 35), it is conceivable that ADAR1 protects against dsRNA-induced apoptosis. To determine if ADAR1 is a general suppressor of apoptosis, we also tested whether ADAR1 protects against cell death induced by two other inducers of apoptosis: TNF-α, an inflammatory cytokine that stimulates apoptosis via the FADD adaptor to activate initiator caspase 8 (36), and staurosporine, a broad kinase inhibitor and inducer of apoptosis (37). PKR[kd], ADAR1[kd], and CON[kd] cells were treated with TNF-α together with cyclohexamide, and cell viability following treatment was measured by MTS assay and PARP cleavage. The percentage of viable cells (Fig. 3*A*, *top*) and the amount of PARP cleavage (Fig. 3*B*, *top*) following treatment with TNF-α/cyclohexamide were similar between PKR[kd] and CON[kd] cells, consistent with previous reports indicating that PKR does not play a role in TNF-α-induced apoptosis (29, 38). Likewise, the percentage of viable cells and the amount of PARP cleavage following TNF-α/cyclohexamide treatment were similar between ADAR1[kd] and CON[kd] cells (Fig. 3, *A* (*top*) and *B* (*top*)). In addition, cell viability and PARP cleavage following staurosporine treatment (Fig. 3, *A* (*bottom*) and B (*bottom*)) were similar in PKR[kd] and ADAR1[kd] compared with CON[kd] cells. These results suggest that PKR enhances and ADAR1 protects against apoptosis induced by some, but not all, triggers.

Caspase Cleavage of ADAR1 p150—Following infection with the C[ko] virus and to a lesser extent V[ko] virus and also upon treatment with TNF-α/cyclohexamide or staurosporine, we detected an additional protein species with our ADAR1 polyclonal antiserum (Figs. 2*C* and 3*B*). This protein migrated at ~120 kDa and is a candidate degradation product of ADAR1 because it was recognized by ADAR1 antiserum and was reduced in amount in the ADAR1[kd] cells (Figs. 2*C* and 3*B*). Since the appearance of this protein correlated precisely with PARP cleavage, we hypothesized that it was a caspase cleavage product of ADAR1 p150. To test this hypothesis, we used the pancaspase inhibitor z-VAD-fmk. Treatment of ADAR1-sufficient cells with this drug prevented accumulation both of the ~120-kDa ADAR1 product and the ~85-kDa PARP cleavage product (Fig. 4), consistent with the conclusion that the novel ADAR1 protein species was a caspase-mediated cleavage product.

ADAR1 Suppresses WT and V[ko] Virus-induced PKR Activation—We showed previously that PKR is activated upon infection with C[ko] virus but not WT or V[ko] virus and that activation of PKR correlated with PKR-dependent measles virus growth inhibition and apoptosis induction (28). We therefore considered the possibility that the enhanced cell death and decreased virus growth observed in ADAR1[kd] cells was due to enhanced PKR activation. To test this hypothesis, we measured PKR phosphorylation using an antibody against phosphothreonine 446. As we previously reported for PKR/ADAR1-sufficient cells (28), very low levels of PKR activation were detected following infection with the WT or V[ko] viruses, but substantial PKR activation by C[ko] virus was observed by 24 h postinfection in these cells (Fig. 5, *lanes 1–7*). In the ADAR1[kd] cells, however, activation of PKR was observed for all three viruses; furthermore, the amount and kinetics of activation were similar to that of the C[ko] virus-induced activation in the CON[kd] cells (Fig. 5, *lanes 8–14*). Activation of PKR correlated with activation of eIF-2α, as measured by phosphorylation of eIF-2α on serine 51, and also with decreased expression of viral proteins hemagglutinin and GFP.

ADAR1 Suppresses IRF-3 Activation by WT and V[ko] Viruses—Because we observed enhanced PKR activation in ADAR1[kd] cells but not ADAR1-sufficient cells upon infection with
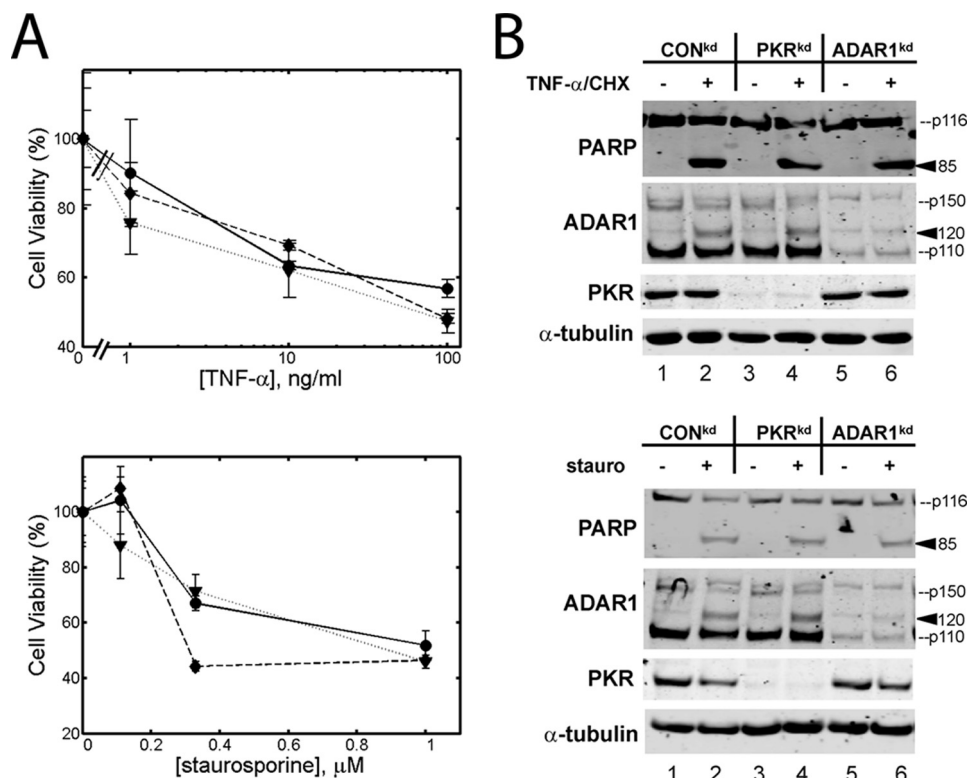
A

B

FIGURE 3. ADAR1 and PKR protein deficiencies do not affect TNF-α or staurosporine-induced apoptosis. *A*, cells were treated with varying concentrations of TNF-α and 1 μg/ml of cyclohexamide (*top*) or staurosporine (*bottom*), and MTS analysis was performed 8 h (TNF-α and cyclohexamide) or 12 h (staurosporine) after treatment. The assay was performed with CON^{kd} cells (*dotted line, triangles*), ADAR1^{kd} cells (*dashed line, diamonds*), and PKR^{kd} cells (*solid line, circles*). The results shown are the means with S.D. values (*n* = 3 for each time point). *B, top*, CON^{kd}, PKR^{kd}, and ADAR1^{kd} cells were treated with 10 ng/ml TNF-α and 1 μg/ml cyclohexamide (+) or left untreated (−), and whole cell extracts were prepared 12 h after treatment. Western immunoblot analyses were performed using the indicated antibodies. *Bottom*, same as the *top panel*, only cells were treated with 0.25 μM staurosporine (*stauro*) (+) or left untreated (−). The *arrowheads* mark the positions of the PARP 85 and ADAR1 120 cleavage products.
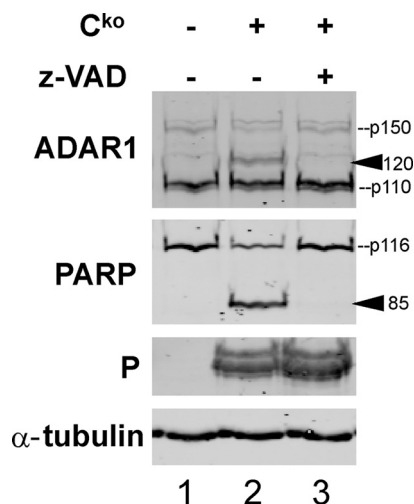

FIGURE 4. Accumulation of the presumed ADAR p150 caspase cleavage product is inhibited by z-VAD-fmk. CON^{kd} cells were infected with C^{ko} virus or left uninfected and were treated with medium alone or medium containing the caspase inhibitor z-VAD-fmk (100 μM) as indicated. Whole cell extracts were made 36 h postinfection, and Western immunoblot analyses were performed using the indicated antibodies. The *arrowheads* mark the positions of the PARP 85 and ADAR1 120 cleavage products.

WT and V^{ko}, we next asked whether activation of additional dsRNA-dependent pathways might also be enhanced in these cells. To test this possibility, we examined IRF-3 activation.

IRF-3 is a key transcription factor for the induction of IFN-β (39). IRF-3 is activated by C-terminal phosphorylation and following activation translocates to the nucleus and mediates transcription (40). IRF-3 is activated by dsRNA-dependent pathways, including those that involve TLR3 (toll-like receptor 3), RIG-I (retinoic-acid-inducible gene I)-like cytoplasmic receptors, and PKR (41–43).

Following infection with the C^{ko} virus, but not the WT or V^{ko} viruses, substantial IRF-3 activation was observed in ADAR1-sufficient CON^{kd} cells (Fig. 6, *top*, *lane 4*), as determined by the appearance of slower migrating IRF-3 species that represent activated IRF-3 and correspond to C-terminal phosphorylation of IRF-3 (41, 44). In the ADAR1^{kd} cells, however, IRF-3 was activated by all three viruses, albeit at different levels (Fig. 6, *top*, *lanes 5–8*). Enhanced phosphorylation of PKR upon infection with each of the three viruses, WT, V^{ko}, and C^{ko}, was again observed in the ADAR1^{kd} cells (Fig. 6, *second panel*, *lanes 5–8*), similar to the findings shown in Fig. 5. These results indicate that ADAR1 enhances IRF-3 activation as well as PKR activation following MV infection.

DISCUSSION

Although biased A-to-I hypermutation in SSPE brains implicates ADAR1 in MV replication (1, 10), the role of ADAR1 in measles virus infection has not been characterized. To test the role of ADAR1 during MV infection, we generated a human cell line stably deficient in ADAR1 that expressed levels of ADAR1 protein 10–15-fold lower than those of the parental cell line that fully supports MV replication. We found that ADAR1 enhances the growth of V^{ko} and C^{ko} virus mutants deleted for the V and C pathogenic factors (Fig. 1). In addition, we observed that ADAR1 protected against apoptosis induced by WT and V^{ko} but not C^{ko} virus (Fig. 2). These results indicate a proviral and antiapoptotic role of ADAR1 during MV infection; in contrast, PKR is antiviral and proapoptotic during MV infection (28). Thus, one enzyme may oppose the other's activity. Indeed, we observed enhanced PKR activation in ADAR1^{kd} compared with ADAR1-sufficient control cells in response to infection with WT and V^{ko} virus.

Enhanced PKR activation in the ADAR1^{kd} cells following infection with WT and V^{ko} virus correlated with enhanced eIF-2α phosphorylation and decreased viral protein expression (Fig. 5). Therefore, PKR-mediated translation inhibition might be responsible for the decreased growth of WT and V^{ko} viruses
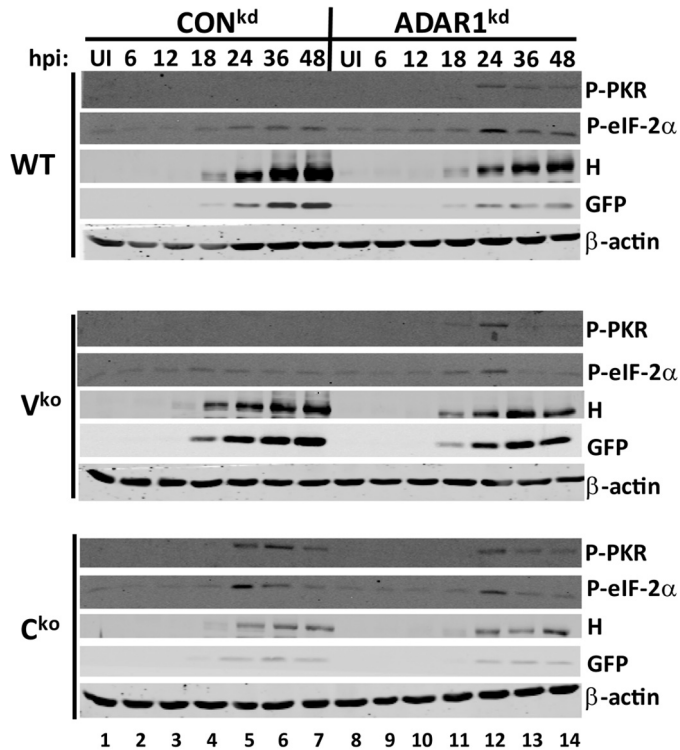
FIGURE 5. **PKR activation is enhanced in ADAR1-deficient cells compared with ADAR1-sufficient cells following infection with WT and V^{ko} but not C^{ko} MV.** CON^{kd} and ADAR1^{kd} cells were infected with WT, V^{ko}, or C^{ko} virus or left uninfected (*UI*). Whole cell extracts were prepared at the indicated times postinfection (*hpi*) and analyzed by Western immunoblot analysis with phospho-PKR (Thr^{446}), phospho-eIF-2α (Ser^{51}), and β-actin antibodies as well as with antibodies against hemagglutinin (*H*) and GFP proteins expressed by MV.
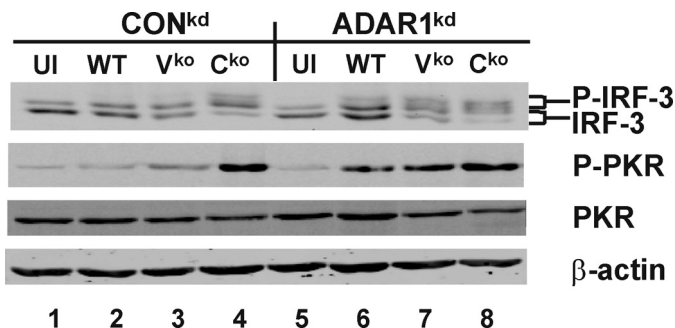

FIGURE 6. **IRF-3 phosphorylation is enhanced in ADAR1-deficient cells compared with ADAR1-sufficient cells following infection with WT and V^{ko} MV.** CON^{kd} and ADAR1^{kd} cells were infected with WT, V^{ko}, and C^{ko} virus or left uninfected (*UI*). Whole cell extracts were prepared 24 h after infection and analyzed by Western immunoblot analysis with antibody against IRF-3, phospho-PKR (Thr^{446}) PKR, and β-actin. The *brackets* indicate the mobility position of non-phosphorylated and C-terminally phosphorylated IRF-3 forms (41, 44).

in the ADAR1^{kd} cells. However, PKR-mediated translation inhibition cannot explain the substantially decreased growth of the C^{ko} virus in the ADAR1^{kd} cells (Fig. 1), since enhanced PKR phosphorylation was not seen in these cells following infection with the C^{ko} virus (Fig. 5). Since C protein has several functions in cells, including control of virus transcription and replication (45, 46) as well as virion assembly and release (47), it is conceivable that ADAR1 affects some other step in the MV replication cycle in addition to protein synthesis.

Our results revealing an antiapoptotic activity for ADAR1 in virus-infected cells are consistent with those obtained with mouse *Adar1* gene disruption studies. *Adar1*$^{-/-}$ mouse embryos die at embryonic day ~12.5 due to severe apoptosis in the liver and defects in hematopoiesis (48, 49). Moreover, mouse embryo fibroblasts derived from *Adar*$^{-/-}$ mice are highly prone to serum-deprived apoptosis (49). However, we observed that ADAR1 did not block cell death triggered by TNF-α or staurosporine (Fig. 3), suggesting that ADAR1 is not a general suppressor of apoptosis. Because ADAR1 is a dsRNA-binding protein with dsRNA editing and destabilizing activity (1, 34, 35), it is likely that ADAR1 selectively protects against cell death induced by dsRNA or another virus-specific RNA signal. If this is correct, then what might be the inducer of apoptosis in the hematopoietic system during embryogenesis in the *Adar1*$^{-/-}$ mouse? It is tempting to speculate that a structured RNA, possibly a microRNA, regulates apoptosis in that system, and ADAR1 impairs the activating activity of this RNA through editing (1, 50).

Upon infection with C^{ko} but not WT measles virus, we observed an ADAR1-related protein product of ~120 kDa. We also observed this product following infection with E3L deletion vaccinia virus but not WT vaccinia virus (data not shown). Since the C^{ko} virus is highly apoptotic compared with WT measles, and likewise E3L deletion vaccinia virus is highly apoptotic compared with WT vaccinia virus (30), we hypothesized that this ADAR1 species might be a caspase cleavage product of ADAR1 p150. Fully consistent with this idea, the appearance of the 120-kDa species correlated with a decrease in ADAR1 p150 levels and with PARP cleavage (Figs. 2*C*, 3*B*, and 4) and furthermore was inhibited by the caspase inhibitor z-VAD-fmk (Fig. 4). The cleavage of ADAR1 by caspases further supports the idea that ADAR1 plays an important role during apoptosis, but the biological relevance of the presumed caspase cleavage product remains entirely unknown.

In addition to PKR activation, we also observed increased IRF-3 activation in the ADAR1-deficient cells following infection with WT and V^{ko} virus (Fig. 6). IRF-3 is a pivotal component of the host antiviral innate response leading to the induction of IFN-β (39, 40). IRF-3 is activated through TLR3 and RLR (RIG-I-like cytosolic receptor) pathways (41–43), which, like PKR, are activated in response to dsRNA. IRF-3 activation, in some cases, is enhanced by PKR (41). Enhanced activation of IRF-3 in ADAR1^{kd} cells, therefore, might indicate that ADAR1 suppresses dsRNA-dependent antiviral pathways, such as TLR3 or RIG pathways. The observation that IRF-3 is enhanced in ADAR1^{kd} cells is intriguing, since enhanced IFN-stimulated gene expression was reported in *Adar*$^{-/-}$ mice during embryogenesis (51).

The p150 form of ADAR1 is an IFN-inducible enzyme, and since IFNs are cytokines with antiviral activity, our results showing enhanced virus growth and reduced activation of antiviral pathways in the presence of ADAR1 seem paradoxical. However, a proviral role for ADAR1 is not unprecedented, since others have found that ADAR1 increases susceptibility to infection with other viruses, including vesicular stomatitis virus (52), human immunodeficiency virus (53–55), and hepatitis delta virus (56). Together with our findings with MV, ADAR1

thus has a positive role in the replication of RNA viruses of three different genome classes, negative-strand linear RNA (rhabdoviridae, paramyxoviridae), positive-strand linear RNA that undergoes reverse transcription (retroviridae), and the single-strand circular RNA delta virus agent. Furthermore, a prominent role for ADAR1 during MV infection is consistent with the frequent detection of regions of A-to-I hypermutation in MV genomes amplified from brains of SSPE patients (27). It is conceivable that these regions of biased hypermutation in MV are the consequence of routine use of ADAR1 by MV as a replication factor. Presumably, MV not only takes advantage of the ability of ADAR to inhibit antiviral pathways, such as PKR and IRF3, but also has mechanisms to avoid frequent A-to-I modification of its genome RNA by ADAR1 during replication.

In conclusion, we report an antiapoptotic and proviral role for ADAR1 during MV infection, and our results imply that these activities of ADAR1 are achieved through suppression of dsRNA-dependent pathways, such as PKR and IRF-3. Our observations suggest that viruses, including MV, might use ADAR1 as a positive replication factor by selectively exploiting the ability of ADAR to suppress dsRNA-dependent and antiviral pathways.

REFERENCES

1. Toth, A. M., Zhang, P., Das, S., George, C. X., and Samuel, C. E. (2006) *Prog. Nucleic Acid Res. Mol. Biol.* **81,** 369–434
2. Samuel, C. E. (2001) *Clin. Microbiol. Rev.* **14,** 778–809
3. Bass, B. L. (2002) *Annu. Rev. Biochem.* **71,** 817–846
4. Seeburg, P. H., and Hartner, J. (2003) *Curr. Opin. Neurobiol.* **13,** 279–283
5. Liu, Y., and Samuel, C. E. (1999) *J. Biol. Chem.* **274,** 5070–5077
6. Liu, Y., Emeson, R. B., and Samuel, C. E. (1999) *J. Biol. Chem.* **274,** 18351–18358
7. Yang, W., Chendrimada, T. P., Wang, Q., Higuchi, M., Seeburg, P. H., Shiekhattar, R., and Nishikura, K. (2006) *Nat. Struct. Mol. Biol.* **13,** 13–21
8. Kawahara, Y., Zinshteyn, B., Sethupathy, P., Iizasa, H., Hatzigeorgiou, A. G., and Nishikura, K. (2007) *Science* **315,** 1137–1140
9. Baczko, K., Lampe, J., Liebert, U. G., Brinckmann, U., ter Meulen, V., Pardowitz, I., Budka, H., Cosby, S. L., Isserte, S., and Rima, B. K. (1993) *Virology* **197,** 188–195
10. Cattaneo, R., Schmid, A., Eschle, D., Baczko, K., ter Meulen, V., and Billeter, M. A. (1988) *Cell* **55,** 255–265
11. Tenoever, B. R., Ng, S. L., Chua, M. A., McWhirter, S. M., García-Sastre, A., and Maniatis, T. (2007) *Science* **315,** 1274–1278
12. Zahn, R. C., Schelp, I., Utermöhlen, O., and von Laer, D. (2007) *J. Virol.* **81,** 457–464
13. Kumar, M., and Carmichael, G. G. (1997) *Proc. Natl. Acad. Sci. U.S.A.* **94,** 3542–3547
14. Luo, G. X., Chao, M., Hsieh, S. Y., Sureau, C., Nishikura, K., and Taylor, J. (1990) *J. Virol.* **64,** 1021–1027
15. Taylor, D. R., Puig, M., Darnell, M. E., Mihalik, K., and Feinstone, S. M. (2005) *J. Virol.* **79,** 6291–6298
16. Liu, Y., George, C. X., Patterson, J. B., and Samuel, C. E. (1997) *J. Biol. Chem.* **272,** 4419–4428
17. Weier, H. U., George, C. X., Greulich, K. M., and Samuel, C. E. (1995) *Genomics* **30,** 372–375
18. Patterson, J. B., and Samuel, C. E. (1995) *Mol. Cell. Biol.* **15,** 5376–5388
19. Herbert, A., Alfken, J., Kim, Y. G., Mian, I. S., Nishikura, K., and Rich, A. (1997) *Proc. Natl. Acad. Sci. U.S.A.* **94,** 8421–8426
20. Kim, U., Wang, Y., Sanford, T., Zeng, Y., and Nishikura, K. (1994) *Proc. Natl. Acad. Sci. U.S.A.* **91,** 11457–11461
21. Patterson, J. B., Thomis, D. C., Hans, S. L., and Samuel, C. E. (1995) *Virology* **210,** 508–511
22. George, C. X., and Samuel, C. E. (1999) *Proc. Natl. Acad. Sci. U.S.A.* **96,** 4621–4626
23. Poulsen, H., Nilsson, J., Damgaard, C. K., Egebjerg, J., and Kjems, J. (2001) *Mol. Cell. Biol.* **21,** 7862–7871
24. Griffin, D. (2007) in *Fields Virology* (Howley, P., Griffin, D., Lamb, R., Martin, M., Roizman, B., and Straus, S., eds) pp. 1551–1585, Lippincott Williams & Wilkins, Philadelphia, PA
25. Garg, R. K. (2002) *Postgrad. Med. J.* **78,** 63–70
26. Cattaneo, R., Schmid, A., Spielhofer, P., Kaelin, K., Baczko, K., ter Meulen, V., Pardowitz, J., Flanagan, S., Rima, B. K., and Udem, S. A. (1989) *Virology* **173,** 415–425
27. Cattaneo, R. (1994) *Curr. Opin. Genet. Dev.* **4,** 895–900
28. Toth, A. M., Devaux, P., Cattaneo, R., and Samuel, C. E. (2009) *J. Virol.* **83,** 961–968
29. Zhang, P., and Samuel, C. E. (2007) *J. Virol.* **81,** 8192–8200
30. Zhang, P., Jacobs, B. L., and Samuel, C. E. (2008) *J. Virol.* **82,** 840–848
31. Devaux, P., von Messling, V., Songsungthong, W., Springfeld, C., and Cattaneo, R. (2007) *Virology* **360,** 72–83
32. Karber, G. (1931) *Naunyn Schmiedeberg's Arch. Pharmacol.* **162,** 480–483
33. Navaratnarajah, C. K., Leonard, V. H., and Cattaneo, R. (2009) *Curr. Top. Microbiol. Immunol.* **329,** 59–76
34. Bass, B. L., and Weintraub, H. (1987) *Cell* **48,** 607–613
35. Rebagliati, M. R., and Melton, D. A. (1987) *Cell* **48,** 599–605
36. Ashkenazi, A., and Dixit, V. M. (1998) *Science* **281,** 1305–1308
37. Rüegg, U. T., and Burgess, G. M. (1989) *Trends Pharmacol. Sci.* **10,** 218–220
38. Abraham, N., Stojdl, D. F., Duncan, P. I., Méthot, N., Ishii, T., Dubé, M., Vanderhyden, B. C., Atkins, H. L., Gray, D. A., McBurney, M. W., Koromilas, A. E., Brown, E. G., Sonenberg, N., and Bell, J. C. (1999) *J. Biol. Chem.* **274,** 5953–5962
39. Panne, D., Maniatis, T., and Harrison, S. C. (2007) *Cell* **129,** 1111–1123
40. Hiscott, J. (2007) *J. Biol. Chem.* **282,** 15325–15329
41. Zhang, P., and Samuel, C. E. (2008) *J. Biol. Chem.* **283,** 34580–34587
42. Uematsu, S., and Akira, S. (2007) *J. Biol. Chem.* **282,** 15319–15323
43. Yoneyama, M., and Fujita, T. (2009) *Immunol. Rev.* **227,** 54–65
44. Lin, R., Heylbroeck, C., Pitha, P. M., and Hiscott, J. (1998) *Mol. Cell. Biol.* **18,** 2986–2996
45. Bankamp, B., Wilson, J., Bellini, W. J., and Rota, P. A. (2005) *Virology* **336,** 120–129
46. Reutter, G. L., Cortese-Grogan, C., Wilson, J., and Moyer, S. A. (2001) *Virology* **285,** 100–109
47. Devaux, P., and Cattaneo, R. (2004) *J. Virol.* **78,** 11632–11640
48. Hartner, J. C., Schmittwolf, C., Kispert, A., Müller, A. M., Higuchi, M., and Seeburg, P. H. (2004) *J. Biol. Chem.* **279,** 4894–4902
49. Wang, Q., Miyakoda, M., Yang, W., Khillan, J., Stachura, D. L., Weiss, M. J., and Nishikura, K. (2004) *J. Biol. Chem.* **279,** 4952–4961
50. Iizasa, H., and Nishikura, K. (2009) *Nat. Immunol.* **10,** 16–18
51. Hartner, J. C., Walkley, C. R., Lu, J., and Orkin, S. H. (2009) *Nat. Immunol.* **10,** 109–115
52. Nie, Y., Hammond, G. L., and Yang, J. H. (2007) *J. Virol.* **81,** 917–923
53. Phuphuakrat, A., Kraiwong, R., Boonarkart, C., Lauhakirti, D., Lee, T. H., and Auewarakul, P. (2008) *J. Virol.* **82,** 10864–10872
54. Clerzius, G., Gélinas, J. F., Daher, A., Bonnet, M., Meurs, E. F., and Gatignol, A. (2009) *J. Virol.* **83,** 10119–10128
55. Doria, M., Neri, F., Gallo, A., Farace, M. G., and Michienzi, A. (2009) *Nucleic Acids Res.*, in press
56. Jayan, G. C., and Casey, J. L. (2002) *J. Virol.* **76,** 12399–12404